ISSN 1512-1461

UDC: 538.9 Condensed matter Physics, Solid state Physics, Theoretical Condensed matter Physics

ZnO LAYERS SYNTHESIZED USING DOCTOR BLADE METHOD TO DETECT ETHANOL, METHANOL AND ACETONE VAPORS AND CO_2 GAS

R.AS.R. Ranasinghe[1], P. .G.D.C.K. Karunarathna[2] and P. Samarasekara[1]
[1] Department of Physics, University of Peradeniya, Peradeniya, Sri Lanka
[2] Department of Nano Science Technology, Wayamba University of Sri Lanka, Kuliyapitiya, Sri Lanka

Abstract:
ZnO films were prepared using doctor blade method starting from commercially available ZnO nanoparticles. The samples were subsequently annealed at 75 ^0C in air for 30 min. XRD and UV-visible absorption spectrums were employed to determine the structural and optical properties of the samples, respectively. According to XRD pattern, a single phase of ZnO was crystallized in thin film form. The gas sensitivity, response time and recovery time of the ZnO samples were measured in ethanol, methanol and acetone vapors and CO_2 gas at the room temperature. The ZnO samples exhibit the highest gas sensitivity in acetone, and the lowest response time in ethanol among the gas and vapors mentioned here. The sheet resistance of ZnO thin films is 0.212 $M\Omega/cm^2$. The crystallite size of ZnO film was 169 nm as calculated from (101) peak in XRD pattern.
Keywords: *ZnO, gas sensitivity, response time, recovery time, XRD. UV-visible spectrum*

1. Introduction:

ZnO is a n-type semiconductor with wide band gap 3.35 eV. ZnO is chemically stable just like all other oxides. ZnO finds potential applications in photocells, gas sensors, photocatalysts, medicine, food, agriculture and cosmetics. Most of metal oxide such as CuO, Fe_2O_3, WO_3, ZnO, SnO_2 and TiO_2 are used as gas sensors due to their excellent adsorption properties. Resistance of metal oxide increases or decrease due to the oxidation or reduction, respectively. Semiconductor samples in different shapes such as nanowires, nanotubes, nanoparticles and nanofilms have been employed to measure the gas sensitivity. Nanowires of NiO, WO_3, ZnO and CuO have been applied to detect ethanol, acetone and H_2S [1-3]. TiO_2 films consisting of nanoparticle size 3-30 nm have been fabricated by a chemically modified sol-gel technique to detect ethanol, methanol, CO and NO_2 at 400 and 500 ^0C [4]. CeO_2-TiO_2 layers synthesized by spin coating technique have been used to detect O_2 at 420 ^0C [5]. Nb doped TiO_2 films prepared using a micro emulsion technique have been applied to detect CO at 650 ^0C [6]. F doped SnO2 prepared by a micro-electromechanical system has been used to detect 100–600 ppm of CO, H_2, C_3H_8, CH_4 [7]. Mn doped ferric oxide (α-Fe_2O_3) films deposited by the doctor blade method have been employed to detect 1000 ppm of acetone vapor, CO_2 gas, ethanol vapor and ammonia gas. The highest gas sensitivity has been obtained for 6% Mn doped ferric oxide for CO_2 gas which is 70.1% at the room temperature, because the optical band gap is lowest at this doping concentration. The highest gas sensitivity of pure ferric oxide has been obtained for acetone vapor at the room temperature which is 49.2% [8]. The gas sensitivity of ferric oxide thin films has been enhanced by adding the commercially available activated carbon nanoparticles. Adding 2% of activated carbon has enhanced the gas sensitivity of the α-Fe_2O_3 layer from 46% to 50.2% at the room temperature [9].

Tungsten oxide (WO_3) films have been used to detect methane and nitric oxide gases. The response and recovery times of WO_3 films depend on the thickness of films. The origin of gas adsorption has been explained using grain boundary control method [10]. The gas sensitivity of ferric oxide films fabricated using spin coating and doctor blade methods depends on the properties of the PEG binder. Ferric oxide films with PEG binder have indicated a higher gas sensitivity, lower response

ISSN 1512-1461

time and lower recovery time for CO_2 gas compared to the films without PEG [11]. The gas sensitivity of ferric oxide thin films in CO_2 gas, acetone, ethanol and methanol vapors has been measured at different operating temperatures from 28 to 200 ^{0}C. The highest gas sensitivity for CO2 gas was observed at 170 ^{0}C [12]. Copper oxide thin films have been synthesized by reactive dc sputtering. The sputtering pressure and the substrate temperature have been increased up to 8.5 mbar and 192 ^{0}C to investigate the effect of sputtering conditions on the gas sensitivity. The film deposited at 192 ^{0}C under 8.5 mbar pressure provides the highest gas sensitivity of 19.26 in CO_2 gas at the room temperature [13]. Pt/SnO2 has been prepared using flame spray pyrolysis to detect CO with low ppm values such as 8 to 50 ppm at 350 ^{0}C [14]. Al doped TiO2 has been fabricated by citrate-nitrate auto combustion method to detect CO (100-500 ppm) at 600 ^{0}C [15]. PdO loaded SnO_2 nanocomposites has been prepared using the screen-printing method to detect CO at 300 ^{0}C [16]. ZnO nanocomposites is also used as a photocatalyst [17]. ZnO has a large excitation binding energy (60 meV) and deep violet/borderline ultraviolet (UV) absorption at the room temperature [18]. ZnO also demonstrates antifouling and antibacterial properties [19]. In addition, the manufacturing cost of ZnO is about 75% lower than that of TiO_2 and Al_2O_3 nanoparticles [20]. The main disadvantage of ZnO is the high recombination rate to use it as a photocatalyst [21].
The gas sensing properties of ZnO thin films in 1000 ppm of acetone, ethanol, methanol and CO_2 gas at the room temperature are explained in this manuscript. The structural, optical and gas sensing properties of ZnO films synthesized by the doctor blade method are delineated here.

2. Experimental:

0.05 g of polyethylene glycol (PEG) was dissolved in 8 ml of distilled water to prepare the binder. Then the PEG solution was stirred at 45 ^{0}C at 300 rpm for 15 min. 1.5 g of ZnO nanoparticles (size 50 nm) manufactured by Aldrich (with purity more than 97%) was mixed with 5 ml of prepared PEG solution and stirred at 600 rpm at 50 ^{0}C for 2 hours. This ZnO solution was applied on a glass plate using the doctor blade method. Thereafter, the ZnO sample was heated at 75 ^{0}C for 30 min.

The samples were fabricated on conductive glass and nonconductive glass substrates for different characterizations. The X-ray diffraction (XRD) patterns of the samples prepared on nonconductive amorphous glass substrates were measured using a Rigaku Ultima IV X-Ray diffractometer with Cu-Kα (λ=1.5406 *Å*) radiation. UV-visible spectrums of the samples synthesized on nonconductive amorphous glass substrates were measured by means of a Shimadzu 1800 UV-Vis spectrophotometer. The sheet resistance was measured by a Jandel model RM3000+.
The gas sensitivity was measured in a custom-made chamber with gas input and output lines. The conductive layer of the center part of the conductive glass plate was removed to prepare the samples for the gas sensitivity measurements, to avoid the current flowing through the conductive glass. Two gold coated copper electrodes touching the edges of the conductive glass plates were use to measure the electric current through the sample. The initial resistance (R_0) of the ZnO sample was measured. Then the sample and a standard resistor with resistance R_0 were connected in series to a dc power supply of 5V as shown in figure 1. The voltage across the standard resistor was measured by a Fluke multimeter model 289 with time. First the vapor or the gas was introduced into the chamber, and voltage measured until it saturated. Once when the voltage was saturated, the air was flown through the chamber, and the voltage was measured with time.

ISSN 1512-1461

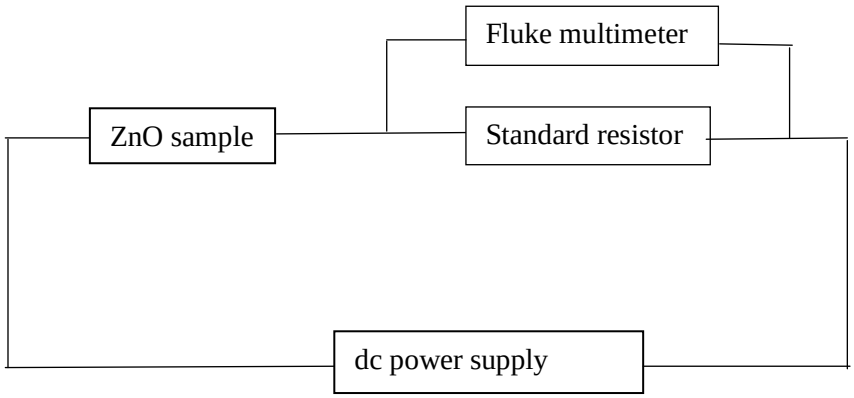

Figure 1: Circuit used to measure the gas sensitivity.

3. Results and discussion:

Figure 2 shows the XRD pattern of the ZnO film with miller indices. All the peaks belong to ZnO indicating that single phase of ZnO was crystallized. The hexagonal wurtzite structure of ZnO was confirmed from file ICSD collection code: 094005 in XRD machine database. This XRD pattern is similar to the powder diffraction pattern of ZnO by implying that the crystallites in the sample are randomly distributed and there is not any preferred orientation of crystallites. The crystallite size (D) calculated from $D = \frac{0.91\lambda}{\beta \cos\theta}$ is 169 nm for (101) peak at 2θ = 36. 25^0. Where β, λ and θ are the full width at half-maxima, the wavelength of X-ray and the angle at (101) peak, respectively. The particle size of used Aldrich ZnO particles is 50 nm. The size of crystallites in the film is higher than the size of used ZnO nanoparticles due to the coalescence of nanoparticles.

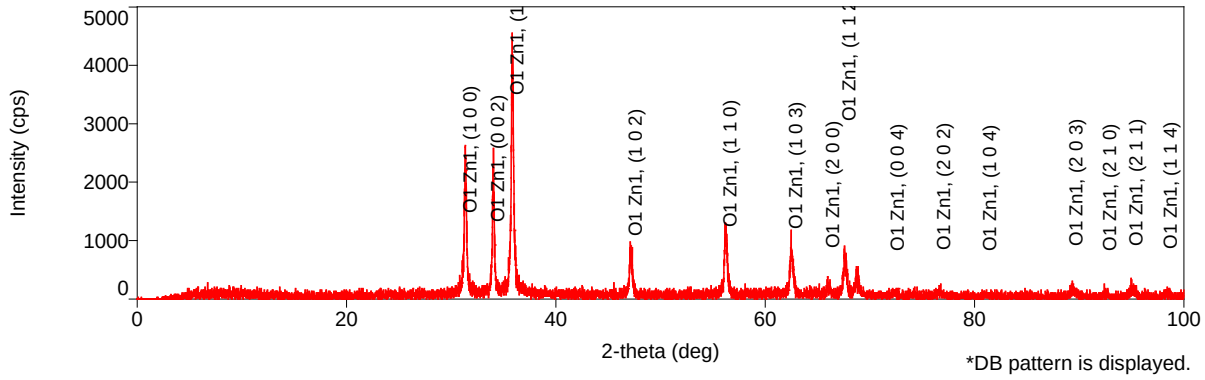

Figure 2: XRD pattern of ZnO film heated at 75 ^{0}C.

Figure 3 shows the UV-visible spectrum of ZnO film. The absorption edge is indicated by the red line. The intercept of red line on horizontal axis of the graph is 395 nm. The corresponding optical band gap is 3.15 eV. This optical band gap is very close to the standard value of the band gap of ZnO by confirming the formation of ZnO in the film. A slight increase of absorption appears at longer wavelengths.

ISSN 1512-1461

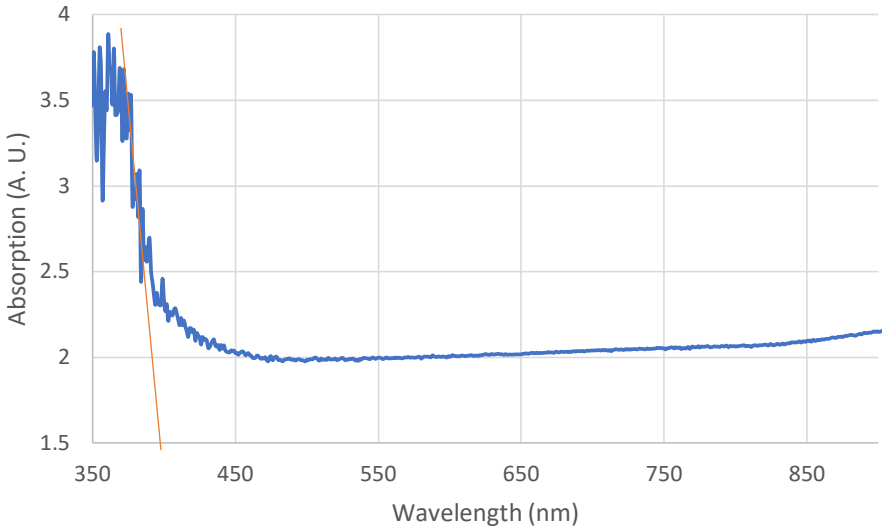

Figure 3: UV-visible spectrum of ZnO film.

Figure 4 shows the voltage versus time graph for ZnO sample measured in 1000 ppm of acetone. The gas sensitivity was calculated from the following equation.

$$Gas\ sensitivity = \frac{R_{gas} - R_0}{R_0} \times 100\%$$

where R_{gas} is the resistance of the ZnO sample, when the ZnO film is saturated after adsorbing the vapor or gas. R_0 is the initial resistance of the ZnO sample, when the ZnO sample is in air. Because this is a series circuit, the same current flows through all the elements. After multiplying the numerator and denominator of the above equation by the electric current,

$$Gas\ sensitivity = \frac{V_{gas} - V_0}{V_0} \times 100\%$$

Here V_{gas} is the voltage across the standard resistor, when the ZnO film is saturated after adsorbing the vapor or gas. V_0 is the initial voltage, when the ZnO sample is in air.
The gas sensitivity, response time and recovery time of the ZnO sample in acetone are 65.5%, 32 min, 6 min, respectively. Initial resistance of this sample between two electrodes was 29 MΩ. The area of all the samples was approximately 1.5x1.6 cm^2.

ISSN 1512-1461

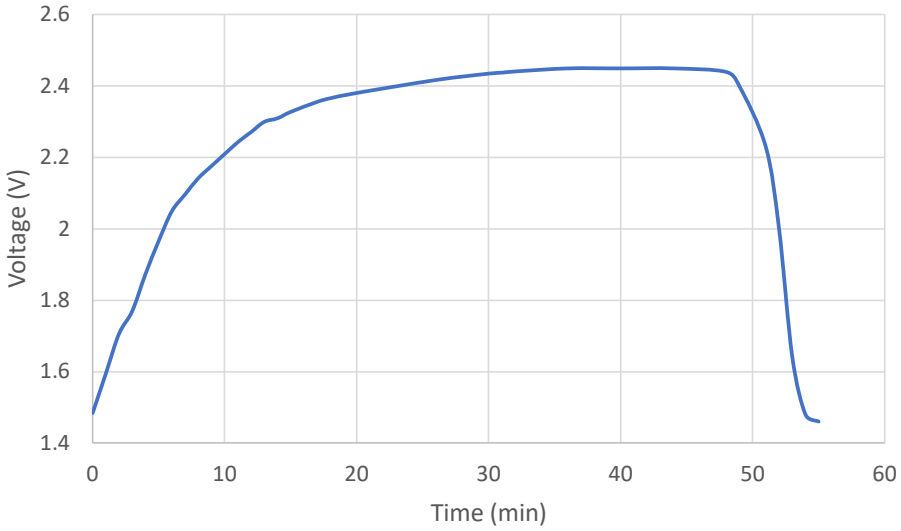

Figure 4: Voltage versus time graph for ZnO sample measured in 1000 ppm of acetone.

Figure 5 represents the voltage versus time graph for the ZnO sample measured in 1000 ppm of ethanol. The gas sensitivity, response time and recovery time of the ZnO sample in ethanol are 23%, 18 min, 15 min, respectively. The ZnO sample responses to ethanol faster than to acetone. However, the gas sensitivity of the ZnO samples in acetone is higher than that in ethanol. Initial resistance of this sample between two electrodes was 15 MΩ.

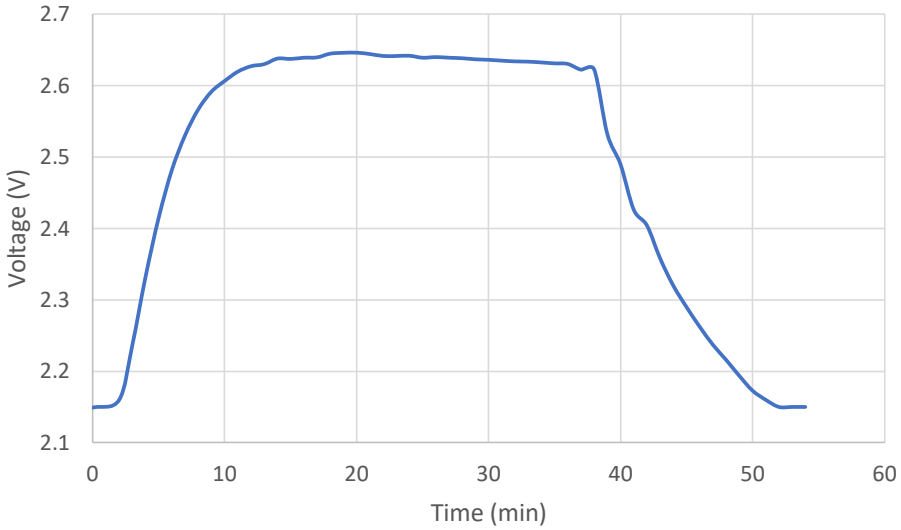

Figure 5: Voltage versus time graph for the ZnO sample measured in 1000 ppm of ethanol.

Figure 6 represents the voltage versus time graph for the ZnO sample measured in 1000 ppm of methanol. The gas sensitivity, response time and recovery time of the ZnO sample in methanol are 20%, 32 min, 12 min, respectively. Initial resistance of this sample between two electrodes was 20 MΩ.

ISSN 1512-1461

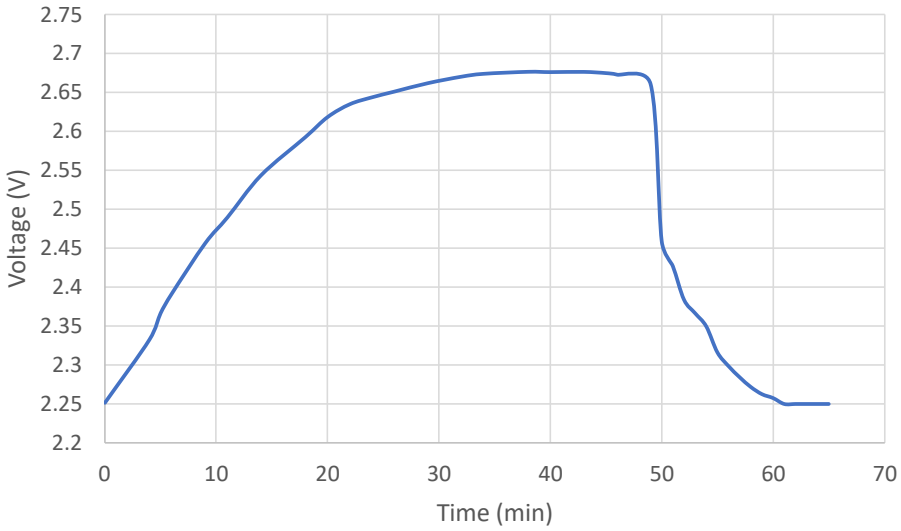

Figure 6: Voltage versus time graph for the ZnO sample measured in 1000 ppm of methanol.

Figure 7 represents the voltage versus time graph for the ZnO sample measured in 1000 ppm of CO_2. The gas sensitivity, response time and recovery time of the ZnO sample in CO_2 are 10%, 4 min, 15 min, respectively. In all these cases, the current of the circuit increases implying that the conductivity of the ZnO sample increases after adsorbing the vapor or the gas. Therefore, the gas or the vapor donates electrons to the ZnO sample.

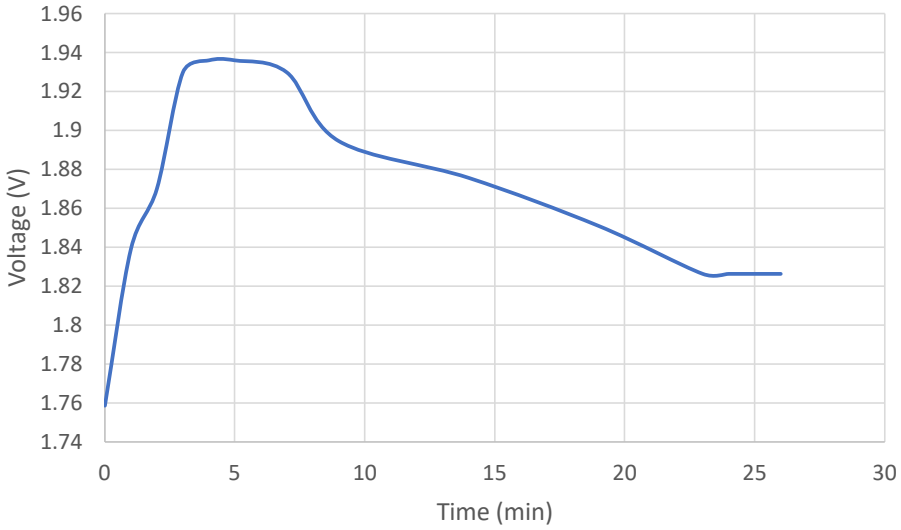

Figure 7: Voltage versus time graph for the ZnO sample measured in 1000 ppm of CO_2.

ISSN 1512-1461

	acetone	ethanol	methanol	CO_2
Gas sensitivity (%)	65.5	23	20	10
Response time (min)	32	18	32	4
Recovery time (min)	6	15	12	15

Table 1: Gas sensitivity, response time and recovery time in different vapors and CO_2 gas.

According to the table 1, the ZnO samples attain the highest sensitivity in acetone and the lowest sensitivity in CO_2. The best response time was found in CO_2. The best recovery time was found in acetone. As expected, the best response time was found for the gas with lowest gas sensitivity [10]. The gas sensitivity of pure ZnO, Al-doped ZnO, In-doped ZnO and Ga doped ZnO have been used to detect ammonia, hydrogen, butane, methane, ethyl alcohol and acetone [22]. However, the dopants have not improved the gas sensitivity in most of these cases. Our undoped ZnO films indicate some reasonable gas sensitivities. ZnO thick films have been applied to detect H_2S, NH_3, LPG and CO_2 [23]. The gas sensitivity of their ZnO films for CO_2 gas is really small compared to that for H_2S. Very high gas sensitivity of ZnO has been measured in very low ppm of ethanol vapor at high operating temperatures [24]. Most of these ZnO films have been deposited on expensive gold micropatterns, silver or platinum to obtain higher gas sensitivity, lower response time and lower recovery time at low ppm of the gas or the vapor [22, 24, 25, 26]. As a result, good electrical contacts have been attained. However, our films were deposited on low-cost conductive glass plates. Therefore, the response and recovery times of our ZnO films are higher compared to the films deposited on expensive highly conductive gold or platinum. As a result, the performance to cost ratio of our samples is higher. Indium doped ZnO films have been employed as CO gas sensors [25]. The highest gas sensitivity was obtained for the 15 wt% In doped ZnO samples, which is about 4.19 at 4 ppm of CO. ZnO films prepared using the screen-printing technique have been applied to detect acetone vapor. The highest gas sensitivity was observed for bisphenoids morphology of ZnO at operating temperature of 400 ^{0}C in 10 ppm of acetone vapor, which is 26.4 [26].

The adsorption of ethanol, methanol, acetone or CO_2 gas decreases the width of the depletion region of ZnO. As a result, the height of Schottky barrier decreases [23, 24]. The energy level diagram for reduction reaction is given in figure 8. Where R is the reducing gas.

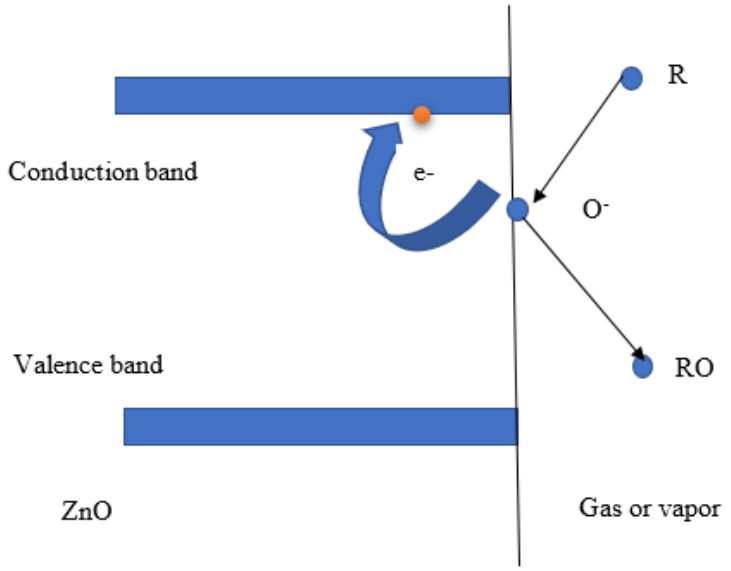

Figure 8: Energy level diagram for gas adsorption.

ISSN 1512-1461

4. Conclusion:

ZnO was crystallized in thin film form starting from the commercially available ZnO powder. Because all these vapors and CO_2 gas donates electrons to ZnO films, the conductivity of ZnO films increases after adsorbing the gas or the vapor. The highest (65.5%) and the lowest (10%) gas sensitivities were obtained for 1000 ppm of acetone and CO_2, respectively. The highest response time (32 min) was measured for acetone and methanol. The ZnO samples quickly response to CO_2 gas compared to other vapors mentioned in this manuscript. Ethanol and CO_2 indicated the highest recovery time, and the acetone showed the lowest recovery time (6 min). Because our samples were deposited on conductive glass substrates, the response and recovery times of our samples were higher compared to the response and recovery times of the gas sensors synthesized on expensive gold, silver or platinum electrical contacts. The optical band gap of ZnO films was found to be 3.15 eV. The resistance of the ZnO films between two electrodes varies in a range from 15 to 29 M for different samples. This variation of the resistance can be attributed to the slight variation of the thickness or the area of the film.

References:

1. N. Kaura, E. Cominia, N. Polia, D. Zappaa and G. Sberveglieria, Procedia Eng. (2015), 120, 760.
2. J. Krainera, M. Delucaa, E. Lacknera, R.W. Teubenbachera, F. Sosadaa, C. Gspanb, K. Rohracherc, E. Wachmannc and A. Koecka, Procedia Eng. (2016), 168, 272.
3. D. Zappaa, E. Cominia and G. Sberveglieria, Procedia Eng. (2012), 47, 430.
4. C. Garzella, E. Comini, C. Frigeri and G. Sberveglieri, Sens. Actuators B (2000), 68, 189.
5. A. Trinchi, Y.X. Li, W. Wlodarski, S. Kaciulis, L. Pandolfi, S. Viticoli, E. Comini and G. Sberveglieri, Sens. Actuators B (2003), 95, 145.
6. T. Anukunprasert, C. Saiwan and E. Traversa, Sci. Technol. Adv. Mater. (2005), 6, 359.
7. C.H. Han, S.D. Hang, I. Singh and T. Toupance, Sens. Actuators B (2005), 109, 264.
8. R.M.T.D.Rajapaksha, P. Samarasekara, P. G. D. C. K. Karunarathna and C. A. N. Fernando, Bulletin of materials science (2021), 44, Article number 182.
9. R.M.T.D.Rajapaksha, P. Samarasekara, P. G. D. C. K. Karunarathna, T.M.W.J. Bandara and C. A. N. Fernando, Ionic research and engineering journals (IRE) (2021), 4(10), 107.
10. P. Samarasekara, GESJ: Physics (2009), 2(2), 44.
11. P. Samarasekara, M.S.P.K. Gunasinghe, P.G.D.C.K. Karunarathna, H.T.D.S. Madusanka and C.A.N. Fernando, GESJ:Physics (2019), 1(21), 7.
12. P. Samarasekara, M.S.P.K. Gunasinghe, P.G.D.C.K. Karunarathna, H.T.D.S. Madusanka and C.A.N. Fernando, GESJ:Physics (2019), 2(22), 3.
13. P. Samarasekara and N.U.S. Yapa, Sri Lankan Journal of Physics (2007), 8, 21.
14. L. Madler, A. Roessler, S.E. Pratsinis, T. Sahm, A. Gurlo, N. Barsan and U. Weimar, Sens. Actuators B (2006), 114, 283.
15. Y.J. Choi, Z. Seeley, A. Bandyopadhyay, S. Bose and S.A. Akbar, Sens. Actuators B (2007), 124, 111.
16. M. Yuasa, T. Masaki, T. Kida, K. Shimanoe and N. Yamazoe, Sens. Actuators B (2009), 136, 99.
17. J.V.S.S.D. Perera, P.G.D.C.K. Karunarathna and P. Samarasekara, STM journals: Journal of Nanoscience, Nanoengineering & Applications (2022), 12(2), 36.
18. K. Choi, T. Kang and S.G. Oh, Mater. Lett. (2012), 75, 240.
19. M. Al-Fori, S. Dobretsov, M.T.Z. Myint et al, Biofouling (2014), 30, 871.
20. S. Liang, K. Xiao, Y. Mo, et al, J. Memb. Sci. (2012), 394–395, 184.
21. C.B. Ong, L.Y. Ng and A.W. Mohammad, Renew. Sustain. Energy Rev. (2018), 81, 536.
22. H. Nanto, T. Minami and S. Takata, J. Appl. Phys. (1986), 60, 482.
23. S. G. Onkar, S. B. Nagdeote, A. S. Wadatkar and Prashant B. Kharat, J. Phys.: Conf. Ser. (2020), 1644, 012060.

ISSN 1512-1461

24. M. Aleksanyan, A. Sayunts, G. Shahkhatuni, Z. Simonyan, G. Shahnazaryan and V. Aroutiounian, Chemosensors (2022), 10, 245.
25. A. Ani , P. Poornesh, K. K. Nagaraja, Gopalkrishna Hegde , E. Kolesnikov , Igor V. Shchetinin, Albin Antony and Suresh D. Kulkarni, J. Mater. Sci: Mater. Electron (2021), 32, 22599.
26. A. Fioravanti, P. Marani, S. Morandi, S. Lettieri, M. Mazzocchi, M. Sacerdoti and M. Cristina Carotta, Sensors (2021), 21, 1331.

Article received 2023-04-19